Available online at www.sciencedirect.com
SCIENCE DIRECT®
International Journal of Heat and Fluid Flow 26 (2005) 256–263
International Journal of HEAT AND FLUID FLOW
www.elsevier.com/locate/ijhff

Transient heat transfer measurements using thermochromic liquid crystal: lateral-conduction error

James R. Kingsley-Rowe [1], Gary D. Lock, J. Michael Owen *

Department of Mechanical Engineering, University of Bath, Bath BA2 7AY, UK

Received 19 January 2004; accepted 4 August 2004
Available online 2 November 2004

Abstract

Thermochromic liquid crystal (TLC) can be used to measure the surface temperature in transient heat transfer experiments. Knowing the time at which the TLC changes colour, hence knowing the surface temperature at that time, it is possible to calculate the heat transfer coefficient, h, and the analytical one-dimensional solution of Fourier's conduction equation for a semi-infinite wall is often used for this purpose. However, the 1D solution disregards lateral variations of the surface temperature (that is, those variations parallel to the surface), which can cause a bias, or lateral-conduction error, in the calculated value of h. This paper shows how the 1D analytical solution can be used to estimate, and to provide a correction for, the error. An approximate two-dimensional analysis (which could be readily extended to three dimensions) is used to calculate the error, and a 2D finite-difference solution of Fourier's equation is used to validate the method.
© 2004 Elsevier Inc. All rights reserved.

1. Introduction

During transient heat transfer experiments, narrow-band thermochromic liquid crystal (TLC) is often used to measure the surface temperature. (Narrow-band is used here for TLC that changes colour over a 1 °C change in temperature; the uncertainty in the measured temperature is typically 0.1 °C.) If the time at which the TLC changes colour is known then the surface temperature can be readily determined and the heat transfer coefficient, h, can be calculated. In most cases, h is calculated from the one-dimensional solution of Fourier's conduction equation for a semi-infinite solid (or wall), and the reader is referred to Jones and Hippensteele (1988), Kasagi et al. (1989), Camci et al. (1991) and Baughn (1995) for more details.

The above transient techniques implicitly assume that h is invariant with time. This is seldom exactly true as h can depend on both the level and distribution of the surface temperature. However, for forced convection, these effects are often insignificant, and the use of two or more narrow-band crystals should reveal their magnitude.

Uncertainties in the measured temperatures will give rise to uncertainties in the calculated values of h, and a means of estimating and minimising these uncertainties is given by Yan and Owen (2002). Another source of error is lateral conduction. The one-dimensional analysis considers only the conduction in the x-direction, normal to the surface of the wall, and conduction in the transverse directions is ignored. If, however, there are large transverse variations of the surface temperature then lateral conduction may be significant, resulting in bias errors in the calculated values of h. Lin and Wang (2002), who solved the 3D Fourier equation numerically, showed that lateral conduction could result in errors in h of 15–20% if the 1D solutions were used. Ling et al. (2003), who also solved the 3D equations numerically, produced a technique that could be used

* Corresponding author. Tel.: +44 1225 386 934; fax: +44 1225 386 928.
E-mail address: j.m.owen@bath.ac.uk (J. Michael Owen).
[1] Present address: Department of Engineering Science, University of Oxford, Oxford, UK.

0142-727X/$ - see front matter © 2004 Elsevier Inc. All rights reserved.
doi:10.1016/j.ijheatfluidflow.2004.08.011

Nomenclature

Bi	(hL/k) Biot number
$\overline{Bi}$	$(\bar{h}L/k)$ corrected Biot number
Bi^*	true value of Biot number
c	constant of proportionality for correction
C_p	specific heat of solid
f	parameter in 1D solution of Fourier's equation
g	parameter in correction of Bi
h	heat transfer coefficient
$\bar{h}$	corrected value of h
k	thermal conductivity of solid
L	wall thickness
q	heat flux normal to surface
t	time
t_p	penetration time
T	temperature of wall
T_0	initial temperature of wall (at $t = 0$)
x	normal coordinate (measured from surface)
y	lateral coordinate

Greeks

α	$(k/\rho C_p)$ thermal diffusivity of solid
β	$(Bi\sqrt{\tau})$ parameter in 1D solution of Fourier's equation
Γ	(τ_0/β_1) bias-amplitude parameter
ε_1	$([(Bi_1 - Bi^*)/Bi^*])$ original nondimensional error in Biot number
$\bar{\varepsilon}$	$([(\overline{Bi} - Bi^*)/Bi^*])$ nondimensional error in Biot number after correction
η	(x/L) nondimensional normal coordinate
λ	(y/L) nondimensional lateral coordinate
θ	$((T - T_0)/(T_{aw} - T_0))$ nondimensional temperature
ρ	density of solid
τ	$(\alpha t/L^2)$ Fourier number
$\bar{\tau}$	$(\tau(1 + \bar{\phi}))$ corrected Fourier number
τ_0	value of τ when TLC changes colour
ϕ	$(\frac{\partial^2\theta}{\partial\lambda^2}/\frac{\partial^2\theta}{\partial\eta^2})$ correction parameter
$\bar{\phi}$	average value of ϕ
ϕ_0	value of ϕ at $\eta = 0$, $\lambda = 0$, $\tau = \tau_0$

Subscripts

aw	adiabatic-wall value
w	value at $x = 0$, $\eta = 0$
1	value corresponding to 1D solution of Fourier's equation

to process TLC measurements in the presence of lateral conduction.

This paper shows how the analytical 1D solution of Fourier's equation can be corrected when lateral conduction is significant. It is demonstrated here for the case of lateral conduction in one direction (the y-direction) but it could be readily extended to the case where there is lateral conduction in the second direction (the z-direction). The advantage of the method is that it uses a modified version of the 1D analytical solution and avoids the need to solve the 2D or 3D finite-difference equations.

Section 2 describes the analysis on which the method is based. Section 3 outlines the numerical method used to solve the analytical equations, and describes the smoothing techniques employed to calculate the surface variations in h. In Section 4, the method is used to calculate the lateral-conduction error for a range of test cases, and the conclusions are summarised in Section 5.

2. Calculation of lateral conduction error

2.1. Fourier's conduction equation

In dimensional form, Fourier's 2D conduction equation can be written as

$$\rho C_p \frac{\partial T}{\partial t} = k\left(\frac{\partial^2 T}{\partial x^2} + \frac{\partial^2 T}{\partial y^2}\right) \tag{2.1}$$

where x is the coordinate measured from the surface of the wall, and normal to it, and y is the transverse coordinate parallel with the surface.

The 1D equation (when $\partial^2 T/\partial y^2 = 0$) has a particularly simple solution for a semi-infinite wall with a step-change in the heat transfer coefficient, h, for which the boundary conditions are

$$\left.\begin{aligned} &T(x,t) = T_0 \quad \text{for } t = 0 \text{ and for all } x \\ &q = -k\frac{\partial T}{\partial x} = h(T_{aw} - T_w) \quad \text{for } x = 0 \text{ and for } t > 0 \\ &T(x,t) = T_0 \quad \text{as } x \to \infty \text{ and for all } t \end{aligned}\right\} \tag{2.2}$$

The solution of the 1D equation is then

$$\theta_w = \frac{T_w - T_0}{T_{aw} - T_0} = f(\beta) \tag{2.3}$$

where

$$f(\beta) = 1 - e^{\beta^2}\,\mathrm{erfc}(\beta) \tag{2.4}$$

and

$$\beta = \frac{h\sqrt{t}}{\sqrt{\rho C_p k}} \tag{2.5}$$

It is more convenient to use the nondimensional form of Fourier's equation in which

$$\theta = \frac{T - T_0}{T_{aw} - T_0}, \quad \eta = x/L, \quad \lambda = y/L, \quad \tau = \alpha t/L^2,$$
$$Bi = hL/k \tag{2.6}$$

Although L is an arbitrary parameter, which has no effect on the solution of Fourier's equation, it is taken here to be the thickness of the wall.

Eq. (2.1) can then be written as

$$\frac{\partial\theta}{\partial\tau} = \frac{\partial^2\theta}{\partial\eta^2} + \frac{\partial^2\theta}{\partial\lambda^2} \tag{2.7}$$

For the 1D case (where $\partial^2\theta/\partial\lambda^2 = 0$), the boundary conditions are

$$\left.\begin{array}{l} \theta = 0 \quad \text{for } \tau = 0 \text{ and for all } \eta \\ \dfrac{\partial\theta}{\partial\eta} = -Bi(1-\theta) \quad \text{for } \eta = 0 \text{ and for } \tau > 0 \\ \theta = 0 \quad \text{as } \eta \to \infty \text{ for all } \tau \end{array}\right\} \tag{2.8}$$

The solution for θ_w, which is the same as Eq. (2.3) is,

$$\theta_w = f(\beta) = 1 - e^{\beta^2}\,\mathrm{erfc}(\beta) \tag{2.9}$$

where

$$\beta = Bi\sqrt{\tau} \tag{2.10}$$

It should be noted that Bi and τ are usually referred to as the Biot number and the Fourier number, respectively. It should also be noted that β is independent of L.

2.2. Approximate solution of Fourier's equation in two dimensions

Define $\phi = \phi(\eta, \lambda, \tau)$ as

$$\phi = \frac{\partial^2\theta}{\partial\lambda^2} \Big/ \frac{\partial^2\theta}{\partial\eta^2} \tag{2.11}$$

It is now assumed that ϕ can be approximated by some average value, $\bar{\phi}$, so that Eq. (2.7) can be simplified to

$$\frac{\partial\theta}{\partial\bar{\tau}} = \frac{\partial^2\theta}{\partial\eta^2} \tag{2.12}$$

where

$$\bar{\tau} = \tau(1 + \bar{\phi}) \tag{2.13}$$

The solution to this quasi-2D equation is then

$$\theta = f(\bar{\beta}) \tag{2.14}$$

where

$$\bar{\beta} = \overline{Bi}\sqrt{\bar{\tau}} \tag{2.15}$$

and

$$\overline{Bi} = \bar{h}L/k \tag{2.16}$$

$\bar{h}$ being the approximate, or corrected, value of the heat transfer coefficient. It follows that

$$\overline{Bi} = Bi_1(1 + \bar{\phi})^{-1/2} \tag{2.17}$$

where Bi_1 is the Biot number obtained from the 1D solution. Thus, if $\bar{\phi}$ can be estimated then an approximation of the correct Biot number can be obtained.

A physical interpretation of this result can be obtained by considering conditions at the point $\eta = 0$, $\lambda = 0$. If $\partial^2\theta/\partial\lambda^2 > 0$ then lateral conduction would cause heat to flow towards that point. In an experiment, this would *reduce* the time for the TLC to change colour, and the 1D solution would consequently *overestimate* the value of the Biot number. Now, as $\partial^2\theta/\partial\eta^2 > 0$ everywhere, it follows from Eq. (2.11), that if $\partial^2\theta/\partial\lambda^2 > 0$ then $\bar{\phi} > 0$; hence, from Eq. (2.17), $\overline{Bi} < Bi_1$. That is, the corrected value of the Biot number would be smaller than the 1D value, which is qualitatively correct. The converse argument applies when $\partial^2\theta/\partial\lambda^2 < 0$, where $\overline{Bi} > Bi_1$.

2.3. Estimation of $\bar{\phi}$

Consider an experiment in which the Biot number is determined at $\eta = 0$, $\lambda = 0$ and $\tau = \tau_0$, where τ_0 is the Fourier number at which the TLC changes colour; ϕ_0 is the value of ϕ at this condition. It is now assumed that

$$\bar{\phi} = c\phi_0 \tag{2.18}$$

where c is a constant of proportionality. As explained in Section 4, c is chosen so as to produce a value of $\bar{\phi}$ that will minimise the lateral-conduction error.

An estimate of ϕ_0 can be found using the 1D solution of Fourier's equation, from which Bi_1 can be determined as a function of λ. From the results of Section 2.1, using the subscript 1 to denote the value corresponding to the 1D solution, it follows that

$$\frac{\partial^2\theta}{\partial\eta^2} = \frac{\mathrm{d}f_1}{\mathrm{d}\beta_1}\frac{\partial\beta_1}{\partial\tau} \tag{2.19}$$

and

$$\frac{\partial^2\theta}{\partial\lambda^2} = \frac{\mathrm{d}f_1}{\mathrm{d}\beta_1}\frac{\partial^2\beta_1}{\partial\lambda^2} + \frac{\mathrm{d}^2 f_1}{\mathrm{d}\beta_1^2}\left(\frac{\partial\beta_1}{\partial\lambda}\right)^2 \tag{2.20}$$

where

$$\frac{\mathrm{d}f_1}{\mathrm{d}\beta_1} = 2[\beta_1(f_1 - 1) + \pi^{-1/2}] \tag{2.21}$$

and

$$\frac{\mathrm{d}^2 f_1}{\mathrm{d}\beta_1^2} = 2[(f_1 - 1)(1 + 2\beta_1^2) + 2\pi^{-1/2}\beta_1] \tag{2.22}$$

As $\beta_1 = Bi_1\sqrt{\tau_0}$, it follows that

$$\frac{\partial\beta_1}{\partial\tau} = \frac{1}{2}Bi_1\tau_0^{-1/2} \tag{2.23}$$

Consequently, from Eq. (2.11),

$$\phi_0 = \frac{2\tau_0}{Bi_1}\left[\frac{\partial^2 Bi_1}{\partial\lambda^2} + g(Bi_1)\tau_0^{1/2}\left(\frac{\partial Bi_1}{\partial\lambda}\right)^2\right] \tag{2.24}$$

where

$$g(Bi_1) = \left[\frac{(f_1-1)(1+2Bi_1^2\tau_0) + 2\pi^{-1/2}Bi_1\tau_0^{1/2}}{Bi_1\tau_0^{1/2}(f_1-1)+\pi^{-1/2}}\right] \tag{2.25}$$

It should be noted that, although Bi_1 and τ_0 depend on L, ϕ_0 is independent of L.

It should be remembered that, as Eq. (2.11) shows, ϕ, and hence the lateral-conduction error, depends on $\partial^2\theta/\partial\lambda^2$: if that term is zero then the error will be zero. Eq. (2.24) shows that ϕ_0 and hence the error, depends on the lateral variation of Bi_1; this *suggests*, paradoxically, that the error depends only on the lateral variation of h and not on the variation of θ. The paradox is resolved by reference to Eq. (2.20), which links the lateral variation of θ with that of Bi_1.

Further insight into ϕ_0 can be gained by expressing Eq. (2.24) in terms of β_1, such that

$$\phi_0 = 2\Gamma\left[\frac{\partial^2\beta_1}{\partial\lambda^2} + g(\beta_1)\left(\frac{\partial\beta_1}{\partial\lambda}\right)^2\right] \tag{2.26}$$

where $g(\beta_1)$ is given by Eq. (2.25) with $Bi_1\tau_0^{-1/2}$ replaced by β_1, and

$$\Gamma = \frac{\tau_0}{\beta_1} \tag{2.27}$$

In effect, Γ is a 'bias-amplitude parameter' which, as shown below, is governed by experimental constraints.

Schultz and Jones (1973) defined the 'penetration time', t_p say, as the time for the temperature of the back surface of the wall, or test section, to change by 1% of that of the front surface (i.e. by 0.01 $(T_w - T_0)$). Their value of t_p was based on the solution of the 1D Fourier equation for the case in which the wall is exposed to a step change in its surface temperature rather than to a step change in the air temperature. If L is the wall thickness then this criterion gives

$$t_p = 0.10\frac{L^2}{\alpha} \tag{2.28}$$

and this estimate of the penetration time is used by many experimenters to provide a time limit for the duration of their transient tests with TLC. Using Eq. (2.28) it therefore follows that

$$\tau_0 \leqslant 0.10 \tag{2.29}$$

if this criterion is used.

In addition, Yan and Owen (2002) have shown that random uncertainties in temperature measurements have a significant effect on the uncertainty in the measurement of h. The temperature uncertainties are, in effect, amplified, and the 'amplification parameter' depends strongly on the value of θ_w used in the experiment. The amplification parameter is a minimum for $\theta_w \approx 0.5$ and, for accuracy, an experimenter should limit the experimental range to $0.3 < \theta_w < 0.7$.

From Eq. (2.9), if $\theta_w = 0.3$, 0.5 and 0.7 then $\beta_1 = 0.352$, 0.769 and 1.64 respectively. In addition, if $\tau_0 \leqslant 0.10$ then, for the above values of β_1, it is necessary that $Bi_1 \geqslant 1.11$, 2.43 and 5.19, respectively. Thus, considerations of penetration time and experimental uncertainty place constraints on τ_0 and Bi_1. It follows, from Eq. (2.27), that for these three values of β_1, $\Gamma \leqslant 0.284$, 0.130 and 0.061, respectively. Also, for a given value of τ_0, $\Gamma \propto Bi_1^{-1}$, so that ϕ_0 decreases as Bi_1 increases.

To calculate $\bar{\phi}$ from ϕ_0 according to Eq. (2.18), the value of c must be known. Values of c can be found from the numerical solution of the 2D version of Fourier's equation, as described below.

3. Numerical model

Fourier's equation was discretised by the Crank–Nicholson method, and the resulting finite-difference equations were solved using a block tri-diagonal-matrix algorithm. Fig. 1 shows the coordinates and boundary conditions of the computational domain.

In an experiment, θ_w is known and τ_0, corresponding to the time at which the TLC changes colour, is measured. In the simulation, θ_w was specified and τ_0 was determined numerically, from which Bi_1 could be calculated. As stated above, Yan and Owen (2002) showed that, to minimise uncertainties in the calculated heat transfer coefficient, a value of $\theta_w \approx 0.5$ should be used in experiments. This value of θ_w was used below for many of the computations, but the effect of θ_w was

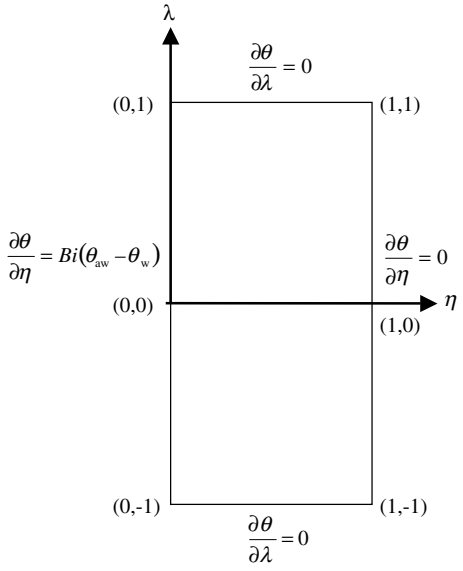

Fig. 1. Computational domain and coordinates.

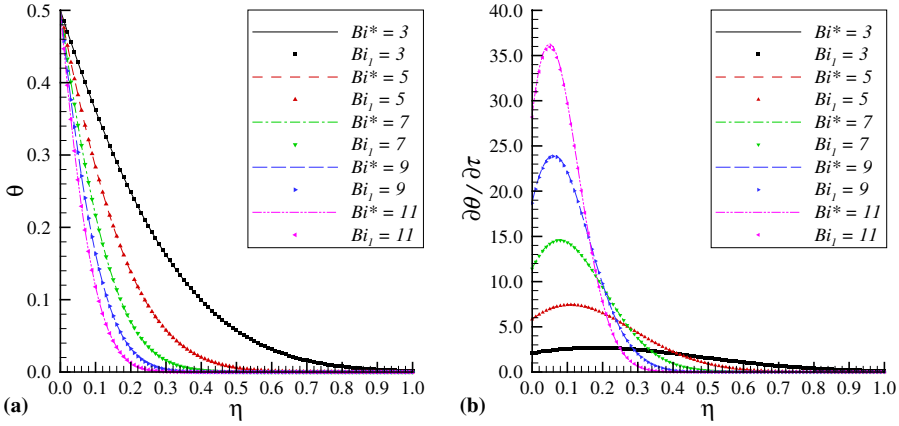

Fig. 2. Comparison between computed and analytical variations of θ and $\partial\theta/\partial\tau$ with η for the 1D case. (Lines represent analytical solutions, and symbols, the numerical solutions.)

considered for $0.3 \leqslant \theta_w \leqslant 0.7$, which covers the sensible range for experiments involving TLC.

From Eq. (2.24) it can be seen that, to evaluate ϕ_0 it is necessary to calculate the first and second derivatives of the Biot number. This was achieved using a least-squares cubic-spline fit of the Biot number as a function of λ (see Numerical Algorithms Group, 2001). The tolerance of the fit is defined as the nondimensional root-mean-square (RMS) error between the data and the smoothing curve. If the tolerance is specified, the algorithm automatically selects the knots for the cubic spline and calculates the appropriate function. Knowing the values of the parameters used in the cubic-spline, the first and second derivatives can be readily determined.

For the computations discussed below, the nondimensional tolerance was taken to be 0.01. This value provided a good fit to the data without producing too many ripples in the calculated derivatives. In practice, some judgement is needed and it is recommended that the lateral variation of the derivatives, particularly $\partial^2 Bi_1/\partial\lambda^2$, should be examined to ensure that the fluctuations are not excessive. If the lateral conduction errors are very large (>20%), it may be necessary to increase the tolerance so as to reduce the fluctuations in the derivatives.

Before solving the 2D version of Fourier's equation, the accuracy of the 1D solution was checked for a range of Biot numbers. The Biot numbers in all the computations were based on a wall-thickness of $L = 10\,\text{mm}$ and a thermal conductivity of $k = 0.2\,\text{W/m K}$. Fig. 2 shows comparisons between the analytical and numerical results, and the agreement for θ and $\partial\theta/\partial\lambda$ versus η can be seen to be good. (It should be remembered that, in the 1D case, $\partial\theta/\partial\tau = \partial^2\theta/\partial\eta^2$.) For these computations, the step lengths of $\Delta\eta$ and $\Delta\lambda$ were taken to be 0.01.

Fig. 3 shows the effect of grid size on the computed variation of τ_0 versus λ for the 2D case, where Bi^* is a function of λ. For both grids, $\eta = 0.01$ and $\Delta\tau = 10^{-4}$; for the fine grid, $\Delta\lambda = 0.01$; for the coarse grid, $\Delta\lambda = 0.05$. As the differences between the two computations were small, the coarse grid was used for all subsequent computations.

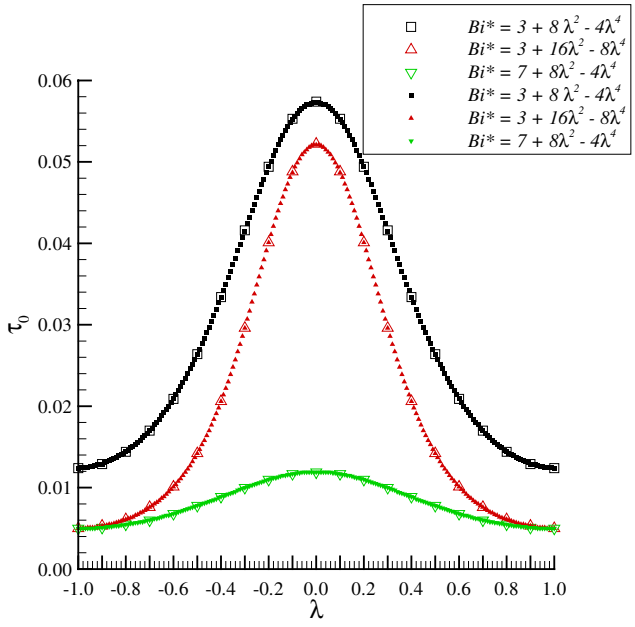

Fig. 3. Effect of grid size on computed variations of τ_0 with λ for the 2D case. (Solid symbols correspond to the fine grid, and open symbols to the coarse grid.)

4. Correction of lateral-conduction error

4.1. Validation for case where *Bi** is known

The validity of the correction given by Eq. (2.17) can be tested if the variation of Bi^* with λ is known. The precise value of ϕ_0 can then be calculated, using Eq. (2.24) with Bi_1 replaced by Bi^*.

The nondimensional errors in the Biot number before and after correction, ε_1 and $\bar{\varepsilon}$ respectively, are defined as

$$\varepsilon_1 = \frac{Bi_1 - Bi^*}{Bi^*} \tag{4.1}$$

and

$$\bar{\varepsilon} = \frac{\overline{Bi} - Bi^*}{Bi^*} \tag{4.2}$$

From the above definitions and Eq. (2.17), it follows that:

$$\varepsilon_1\left(1+\frac{1}{2}\varepsilon_1\right) = \bar{\varepsilon}\left(1+\frac{1}{2}\bar{\varepsilon}\right) + \frac{1}{2}\bar{\phi}\left(1+2\bar{\varepsilon}+\bar{\varepsilon}^2\right) \tag{4.3}$$

As $\bar{\varepsilon}^2 \ll 1$, then

$$\varepsilon_1 - \bar{\varepsilon} \approx \frac{1}{2}\bar{\phi}\frac{1+2\bar{\varepsilon}}{1+\frac{1}{2}(\varepsilon_1+\bar{\varepsilon})} \tag{4.4}$$

In the limit, as $|\bar{\varepsilon}|$ and $|\varepsilon_1|$ tend to zero,

$$\varepsilon_1 - \bar{\varepsilon} \approx \frac{1}{2}\bar{\phi} \tag{4.5}$$

A value of $\bar{\phi}$ can be chosen to minimise $\bar{\varepsilon}$, from which the optimum value of c can be found.

An example is presented in Fig. 4, which shows the variation of Bi^*, Bi_1 and $\overline{Bi}$ versus λ for the case where Bi^* is a polynomial function of λ, with c arbitrarily set equal to 0.25. It can be seen that this value of c produces values of $\overline{Bi}$ that are significantly closer to Bi^* than are the values of Bi_1. The variations of ε_1 and $\bar{\varepsilon}$ with λ for the above case are shown in Fig. 5, and it can be seen that the maximum value of $\bar{\varepsilon}$ is less than 1% compared with a maximum value of ε_1 of over 12%.

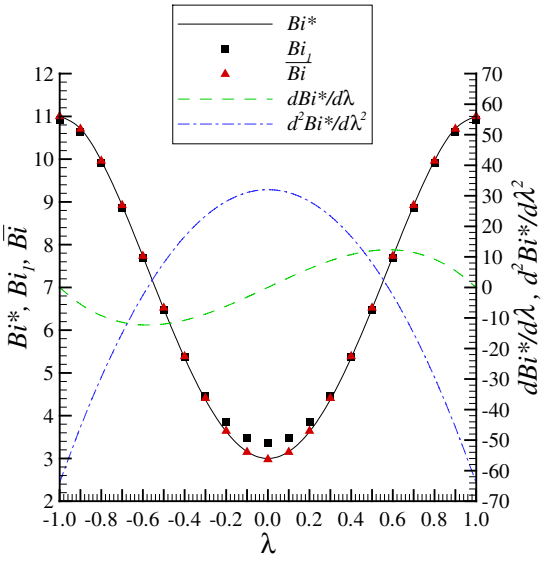

Fig. 4. Comparison between variation of Bi_1, $\overline{Bi}$ and Bi^*, and its derivatives, with λ. (Lines represent analytical solutions, and symbols, the numerical solutions.)

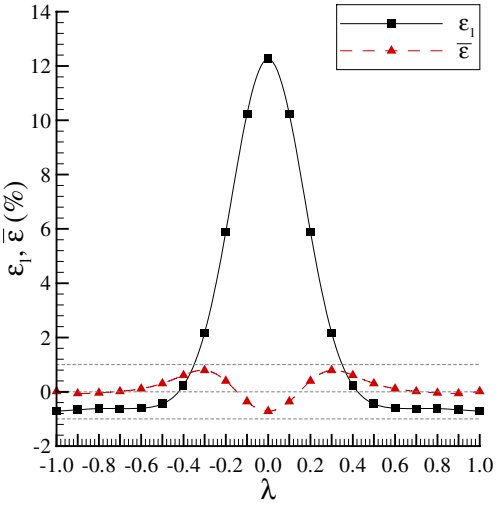

Fig. 5. Variation of ε_1 and $\bar{\varepsilon}$ with λ for the case considered in Fig. 3.

4.2. Testing the method

For the following cases, Bi^* was a known polynomial function of λ, and the error was calculated at $\lambda = 0$. Using Bi_1 to compute the correction, it was found that the optimum value of c depends on both θ_w and ε_1 as shown in Fig. 6 for $0.3 \leqslant \theta_w \leqslant 0.7$ and $\varepsilon_1 \leqslant 40\%$. As ε_1 is not known *a priori*, it is convenient to approximate c as a function of θ_w. For simplicity, the following linear approximation was used over the ranges $0.3 \leqslant \theta_w \leqslant 0.7$ and $5\% \leqslant |\varepsilon_1| \leqslant 40\%$:

$$c = 0.563 - 0.371\theta_w \tag{4.6}$$

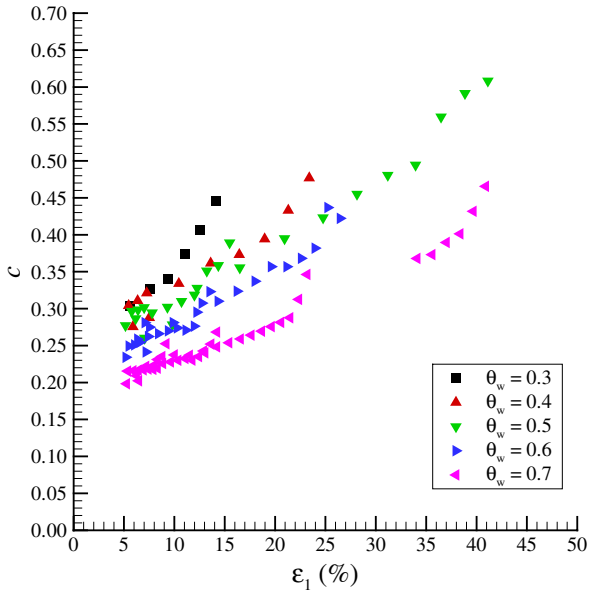

Fig. 6. Effect of θ on variation of c with ε_1.

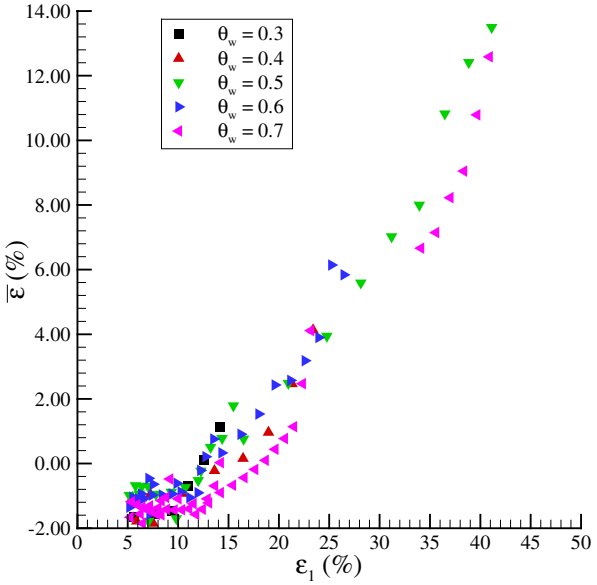

Fig. 7. Effect of θ on variation of $\bar{\varepsilon}$ with ε_1.

For example, for $\theta_w = 0.5$, $c = 0.378$, which corresponds to the value of c shown in Fig. 6 for $\varepsilon_1 \approx 20\%$.

As Eq. (2.9) shows, the 1D solution of Fourier's equation is a function of β_1. The range of validity for β_1 (and hence of h) is implicitly given by the range $0.3 \leqslant \theta_w \leqslant 0.7$, which corresponds to $0.352 \leqslant \beta_1 \leqslant 1.64$.

Using Eq. (4.6) for c, $\overline{Bi}$ can be found from Eqs. (2.17) and (2.18). In the cases considered here, where Bi^* is known, $\bar{\varepsilon}$ can be calculated from Eq. (4.2), and Fig. 7 shows the computed variation of $\bar{\varepsilon}$ with ε_1. Despite the approximations used in the corrections, it can be seen that the error after correction, $\bar{\varepsilon}$, is significantly smaller than the original error, ε_1. For example, for $\theta_w = 0.5$ and $\varepsilon_1 = 20\%$, $\bar{\varepsilon} \approx 2\%$.

It is considered that the method described here can be used to estimate and correct the lateral conduction error in transient experiments using TLC. It may be possible to improve the method by, for example, iteration, but in the authors' opinion this is unnecessary.

4.3. Using the method

The following procedure is suggested.

(1) Using Eqs. (2.9) and (2.10), the lateral variation of Bi_1 is calculated from the TLC measurements.
(2) Using the least-squares cubic-spline smoothing technique described in Section 3, the calculated values of Bi_1 are smoothed.
(3) Using the parameters for the cubic-spline fit, values of $\partial Bi_1/\partial\lambda$ and $\partial^2 Bi_1/\partial\lambda^2$ are calculated at discrete values of λ.
(4) Using these derivatives, ϕ_0 is calculated from Eq. (2.24).
(5) Using Eqs. (2.18) and (4.6), $\bar{\phi}$ is calculated.
(6) Using Eq. (2.17), $\overline{Bi}$ is calculated.

5. Conclusions

If Fourier's 1D conduction equation is used to calculate the Biot number in transient heat transfer experiments then a bias, or lateral-conduction error, can occur. This error depends on the magnitude of the lateral second derivative in the temperature distribution, which in turn depends on the lateral first and second derivatives of the Biot number. Using this fact, an approximate correction has been developed to provide an improved estimate for the Biot number. In the method, the lateral distribution of Biot number (resulting from the solution of Fourier's 1D equation) is smoothed and the surface derivatives are calculated. From these derivatives, an improved estimate of the Biot number is obtained.

The method has been tested numerically for a range of nondimensional temperatures, $0.3 \leqslant \theta_w \leqslant 0.7$ and for uncorrected errors up to 40%; these cover the ranges of sensible experiments with TLC. The errors in the corrected Biot number are significantly reduced; for the important practical case of $\theta_w = 0.5$, an original error of 20% was reduced to 2% after the correction had been applied.

The advantage of the method for transient experiments involving narrow-band TLC is that it uses a modified version of the 1D analytical solution of Fourier's equation and avoids the need to solve the 2D or 3D finite-difference equations. Although the method has only been tested for the case where the surface temperature varies in one dimension, there appears to be no reason why it should not work for 2D variations of temperature.

References

Baughn, J.W., 1995. Liquid crystal methods for studying turbulent heat transfer. Int. J. Heat Fluid Flow 16, 365–375.

Camci, C., Kim, K., Hippensteele, S.A., 1991. A new hue-capturing technique for the quantitative interpretation of liquid crystal images used in convective heat transfer studies. ASME Paper No. 91-GT-122.

Jones, T.V., Hippensteele, S.A., 1988. High-resolution heat-transfer-coefficient maps applicable to compound-curve surfaces using liquid crystals in a transient wind tunnel. NASA Technical Memorandum 89855.

Kasagi, N., Moffat, R.J., Hirata, M., 1989. Liquid crystals. In: Yang, W.J. (Ed.), Handbook of Flow Visualisation. Hemisphere, New York.

Lin, M., Wang, T., 2002. A transient liquid crystal method using a 3-D inverse transient conduction scheme. Int. J. Heat Mass Transfer 45, 3491–3501.

Ling, J.P.C.W., Ireland, P.T., Turner, L., 2003. A technique for processing transient heat transfer liquid crystal experiments in the presence of lateral conduction. ASME Paper No. GT2003-38446.

Numerical Algorithms Group, 2001. NAG Fortran Library Manual: Mark 20. NAG Fortran Library Chapter Introduction E02—Curve and Surface Fitting, Numerical Algorithms Group, Oxford.

Schultz, D.L., Jones, T.V., 1973. Heat transfer measurements in short duration hypersonic facilities. Agardograph 165.

Yan, Y., Owen, J.M., 2002. Uncertainties in transient heat transfer measurements with liquid crystal. Int. J. Heat Fluid Flow 23, 29–35.